Solar Energy Materials and Solar Cells xxx (xxxx) xxx–xxx

Contents lists available at ScienceDirect

Solar Energy Materials and Solar Cells

journal homepage: www.elsevier.com/locate/solmat

On the origin of band-tails in kesterite

G. Rey[a,*], G. Larramona[b], S. Bourdais[b], C. Choné[b], B. Delatouche[b], A. Jacob[b], G. Dennler[b], S. Siebentritt[a]

[a] Laboratory for Photovoltaics (LPV), Physics and Materials Science Research Unit, 41 rue du Brill, L-4422 Belvaux, Luxembourg
[b] IMRA Europe S.A.S., 220 rue Albert Caquot, 06904 Sophia Antipolis, France

ARTICLE INFO

Keywords:
Kesterite
Band-tail
Photoluminescence
CZTSe
CZTSSe

ABSTRACT

Kesterite $Cu_2ZnSn(S_xSe_{1-x})_4$ is an attractive earth-abundant material for low-cost thin film photovoltaics with the capability to achieve power production in the terawatt range and therefore to supply a significant part of the global electricity needs. Despite its advantageous optical and electrical properties for photovoltaic applications, the large band tailing causes voltage losses that limit the efficiency of kesterite-based devices. Here we show that the band-tailing originates mainly from band-gap fluctuations attributable to chemical composition variations at nanoscale; while electrostatic fluctuations play a lesser role. Absorption measurement reveal that the Cu-Zn disorder, always present in kesterite $Cu_2ZnSn(S_xSe_{1-x})_4$, is not the main source of the large band tailing. Instead defect clusters having a significant impact on the band-edge energies, e.g. $[2Cu_{Zn}^{-} + Sn_{Zn}^{2+}]$, are proposed as the main origin for the kesterite band tail.

1. Introduction

Photovoltaics (PV) provides already more than 1% of the global electricity production, with 7–8% in some countries and with a worldwide increasing trend [1]. Cost-competitiveness is the most important criterion to ensure further extensive PV deployment. This translates to the need of low-cost, large-scale and high throughput PV technology, ideally based on earth-abundant and non-toxic material. Kesterite materials, $Cu_2ZnSn(S_xSe_{1-x})_4$ (CZTSSe), has been seen as promising semiconductor for PV [2–4], taking advantage of the large abundance of its metallic constituents, of its direct band-gap [5], adjustable in the 1–1.5 eV range by sulfo-selenide alloying [6–8] leading to intense solar light absorption [9], of favourable transport and doping behaviour [10,11] and of the possibility to grow this semiconductor with large grain at moderate temperature [12]. These properties allowed to achieve solar cells with power conversion efficiencies close to 13% [13]. However, in comparison to other thin-film PV technologies i.e. CIGS (best efficiencies 22.6% [14]) and CdTe (22.1% [15]), kesterite-based PV still shows lower conversion efficiencies limited by both open-circuit voltage (V_{oc}) and fill factor [4,16,17]. Thus, it is essential to understand: what is the main source of recombination to further improve the efficiency of kesterite solar cells. Several mechanisms might be responsible for the increased recombination of kesterite-based devices: those related to the hetero-junction partner and buffer [18,19], to non-ohmic contacts [20,21], grain-boundaries [22,23] or secondary phases [24]. However, the most fundamental loss mechanisms are related to the intrinsic properties of kesterite bulk: due to native deep defects acting as recombination centres [25] or the presence of band-tails [26], limiting the useful energy of photo-generated carriers and their transport. It has been argued that tail states reduce the open circuit voltage only slightly. However, this is only true in the case where radiative recombination is the dominating recombination path [27], whereas tail states also contribute to Shockley-Read-Hall recombination [28], thereby further reducing the room temperature V_{oc} [29].

Tail states are caused by two known fundamental mechanisms [4,30]: either a high concentration of defects combined with a high degree of compensation, which cause the electrostatic potential to fluctuate; or crystalline or compositional inhomogeneities which cause the band-edges and consequently the band-gap to fluctuate.

A potential cause for band-gap fluctuations and electrostatic potential fluctuations in kesterite is the occurrence of Cu-Zn disorder [31,32]. The kesterite material undergoes a Cu-Zn order-disorder transition which is a second order transition. As depicted in Fig. 1, under thermal excitation, Cu and Zn atoms, located in the planes at $z = \frac{1}{4}$ and $\frac{3}{4}$ in the unit cell, can exchange position at low energy cost [25,33–35], because of the similar size of the cations. Therefore, the critical temperatures T_c of the transition are low i.e. 200 °C for pure selenide kesterite (CZTSe) [36] or Se-rich CZTSSe [37] and 260 °C for pure sulphide [31,38]. On the one hand, the band-gap of the material

* Corresponding author.
E-mail address: germrey@gmail.com (G. Rey).
URL: http://www.germain.rey@uni.lu (G. Rey).

https://doi.org/10.1016/j.solmat.2017.11.005
Received 18 July 2017; Received in revised form 9 October 2017; Accepted 3 November 2017

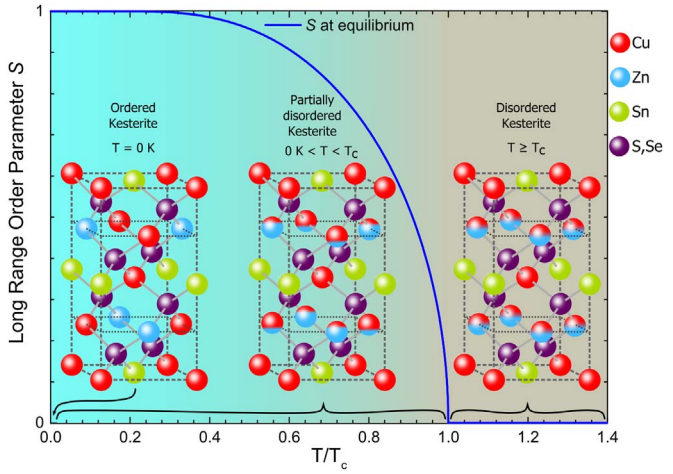

Fig. 1. Illustration of the ordered, Cu-Zn partially ordered and Cu-Zn fully disordered kesterite structure. The plot shows the evolution of the long range order parameter (S) at equilibrium versus the reduced temperature ($\frac{T}{T_c}$) as given by the Bragg and Williams equation $S = \tanh(ST_c/T)$ [42].

depends on the Cu-Zn order state [36,39] and may induce band-gap fluctuations. On the other hand, it is theoretically predicted that Cu_3SnS and $CuZn_2SnS$ S-centred tetrahedral motifs, resulting from Cu-Zn disorder, can cluster in charged nanodomains leading to band-tails induced by fluctuating electrostatic potential [33]. Also clusters of Zn^{+}_{Cu} antisites have been observed by scanning transmission electron microscopy [40].

Although the effects of the Cu-Zn disorder on the crystalline structure, band-gap energy and vibrational properties are well documented, its real impact on the band-tail is still not clarified. The question therefore arises: is the Cu-Zn disorder the main responsible for the large kesterite band tailing? That question has serious implications for the interest in kesterite for PV. Because of the low critical temperature of the Cu-Zn order-disorder transition, kesterite materials always show a significant Cu-Zn disorder [41]. Consequently, it would be an intrinsic limitation of the material if the band tails would mainly result from the Cu-Zn disorder.

In the present work, we investigate the origin of the band tailing in kesterite. First, we determine the nature of the fluctuation that are responsible for the large band tailing in kesterite, which is yet not clarified [43], by investigating the photoluminescence (PL) versus temperature and excitation intensity of high quality CZTSSe (leading to solar cell efficiency above 9%). The behaviour of the spectral broadening with excitation intensity at low temperature (6 K) points out band-gap fluctuations, as opposed to electrostatic potential fluctuations, as the most important cause of the band tailing in kesterite. Therefore, we measure the absorption coefficient (α) spectrum of CZTSSe and CZTSe by spectrophotometry (SP) and PL to be able to measure band tail induced absorption with a high dynamic range. Identical kesterite samples were thermally treated either to induce Cu-Zn disorder or to reduce the Cu-Zn disorder. The comparison of absorption spectra did not reveal any differences in terms of band tailing for Cu-Zn disordered kesterite and partially Cu-Zn ordered kesterite despite the effort in reaching high degree of Cu-Zn order. Both investigations tend to confirm that the large kesterite band tails do not result directly from band-gap variation due to the Cu-Zn disorder.

2. Experimental details

2.1. Sample preparation and post-treatment

CZTSe samples were deposited on Mo-coated soda lime glass substrates heated at 470 °C by co-evaporation of Cu, Zn, Sn, SnSe and Se in a molecular beam epitaxy system. The co-evaporation process was divided in two main steps: first all elements were supplied to form the kesterite, then only Sn, SnSe and Se were supplied to improve crystal quality and prevent Sn- and Se-loss. The samples were terminated with a Zn-rich surface. Se was supplied during final cool-down down to 200 °C. This co-evaporation process is detailed in Ref. [44]. The film composition determined by energy-dispersive X-ray spectroscopy was Cu-poor and Zn-rich (CZTSe#1: Cu/(Zn + Sn) = 0.82, Zn/Sn = 1.10 and CZTSe#2: Cu/(Zn + Sn) = 0.87, Zn/Sn = 1.15).

CZTSSe samples were fabricated as follows. CZTS layers were deposited on Mo glass substrates by non-pyrolytic spraying inside a N_2-filled glove box, using an additive-free water-ethanol (90–10 vol%) based ink of a Cu-Zn-Sn sulphide (no Se) colloid of ~ 10 nm size primary particles, as described in Ref. [45]. The as-sprayed films were submitted to a two-step annealing process: a first annealing step in inert (N_2) atmosphere, allowing to grow the precursor particles from nanometer up to micrometer size, and a second annealing step in Se vapor containing atmosphere allowing both the incorporation of Se (replacing the S) and the curing of the secondary phases present after the first annealing step, as described in Ref. [46]. The Se content of the films was around 60–70% atomic of the total amount (S + Se). The Cu/Zn/Sn ratio in the metal precursors was off-stoichiometric: 1.7/1.1/1 for the CZTSSe#1 and CZTSSe#3 series, 1.9/1.2/1 for the CZTSSe#2 series.

For CZTSe#1 samples, the optional post-synthesis treatments were carried out in a tube furnace filled with N_2 at atmospheric pressure. For CZTSSe samples and CZTSe#2 samples, the optional post-synthesis treatments were performed on a hot plate inside a N_2-filled glove box. The thermal quenching was carried out either by transferring the sample to a cold part of the tube furnace and actively cooling under N_2 flux at room temperature or by transferring the samples from the hot plate to a room temperature holder

2.2. Material characterisation

To perform normal incidence transmittance ($\mathscr{T}$) and 8° incidence reflectance ($\mathscr{R}$) measurements, kesterite thin films were mechanically transferred on glass or quartz substrate using transparent epoxy. The transmittance and reflectance were measured with an UV–vis–NIR dual beam spectrophotometer equipped with a 150 mm integrating sphere. $\mathscr{T}$ and $\mathscr{R}$ were analysed in the framework of the transfer matrix method to extract the complex refractive index ($n + ik$).

Temperature and intensity dependent PL measurement were conducted on a standard CZTSSe#1 sample (neither ordering treatment or disordering treatment) covered with CdS. The sample was placed in a continuous flow cryostat cooled with helium in which the temperature was controlled by a heating stage. A 660 nm diode laser was used for sample excitation. The laser light went through a narrow band-pass filter and a short-pass filter to remove laser harmonics. The excitation was varied by adjusting the laser power (1–100 mW) and using optional calibrated grey filters (OD1-OD4). The laser light was focused on the sample in a 0.1 mm radius spot using a lens. The PL signal was collected by parabolic mirrors. The collected light went through an 850 nm long-pass filter to remove laser reflection and the intensity of the PL signal was optionally attenuated using an OD2 calibrated grey filter. The PL signal was measured by a monochromator coupled with an InGaAs camera. The spectral response of the system was corrected using a calibrated reference lamp. Some measurement artefacts might be seen in the PL spectra due to water absorption around 0.9 eV.

The absorption coefficient measurements by PL, were done on samples prepared similarly as for spectrophotometry measurements (except for the CZTSe#1 series where the PL was measured on thin films deposited Mo-coated glass and covered with CdS). The PL system is the same as described previously except that the laser light was not focused using a lens to obtain a laser spot larger than the PL signal collection area such that the illumination can be considered homogeneous within the sample part from which the PL signal is recorded. In